A. The first type includes those differences that are caused by the different steric and electronic requirements of the ligands. These would include differences in L-Mo-L bond angles and slight differrences in Mo-L bond distances.

B. The second type includes those differences that are the manifestation of distortional isomerism. On the basis of Weighardt's study of distortional isomers of $WOCl_2L^+$, these differences are limited mainly to the M-O and $M-L_{trans\text{-}to\text{-}O}$ distances. From our study of $MoO(NCO)_2(PEt_2Ph)_3$, we conclude that changes in the orientation of the organic groups on the phosphine ligands may cause minor changes in some bond distances and angles (like those described in A above) but that these changes do not necessarily lead to distortional isomers. Although we did not find a blue $MoOX_2L_3$ molecule with a short Mo-O distance in this case, we still feel that such a molecule might exist.

Conclusion

The cocrystallization of two conformers of blue $MoO(NCO)_2(PEt_2Ph)_3$, which differ in the arrangement of the organic groups about the phosphorous atoms but not in Mo-O distance, complements Wieghardt's findings that the difference between distortional isomers of MOL_5'' compounds lies in different M-O and $M-L_{trans\text{-}to\text{-}O}$ distances and not in the orientation of the ligands. The structure of $MoOCl_2(PMePh_2)_3$ is noteworthy as it is a green $MoOX_2L_3$ compound with a short Mo=O bond. Distortional isomerism in MOL_5'' systems has previously been seen only in the few cases that isomers of different colors (blue and green) have been observed. While we present no direct evidence for other complexes for which two isomers exist, our finding of a short Mo=O bond in a green $MoOX_2L_3$ complex suggests that distortional isomerism in these compounds might not be limited to cases in which isomers of different colors are observed. However, whether distortional isomers of these compounds can be prepared and identified as such remains to be seen.

Acknowledgment. We are grateful to the Robert A. Welch Foundation (Grant No. A-494) for financial support. M.P.D. is a National Science Foundation Predoctoral Fellow and also holds a Texaco/IUCCP Fellowship from this department.

Registry No. **1**, 109362-28-9; **2**, 109428-74-2.

Supplementary Material Available: Tables of anisotropic displacement parameters, complete bond distances and angles, and final atomic positional and isotropic equivalent displacement parameters for the nonessential carbon atoms on the phenyl rings for both structure determinations (12 pages); listings of observed and calculated structure factors (37 pages). Ordering information is given on any current masthead page.

Contribution from the Department of Chemistry, Georgetown University, Washington, D.C. 20057

Bonding and Electronic Structure of Conducting Mercury Networks: $KHgC_{4n}$ Graphite Amalgams and Hg_3MF_6 Layers and Chains

Miklos Kertesz*† and Arnold M. Guloy

Received February 4, 1987

Linear chains, close-packed layers, and honeycomb networks of Hg are found in several highly conducting materials. For positively charged Hg systems it is the layers and chains that are calculated to be more stable, whereas for negatively charged ones it is the honeycomb network that is found to be more stable, in agreement with experiments. The electronic structures of these compounds exhibit high densities of states around the Fermi level explaining some of their unusual properties. The small degree of orbital mixing between graphite and the amalgam layer in the graphite compound on the one hand and between Hg and the anions in the linear-chain and layer compounds on the other hand permits a simple interpretation of the results, which is based on a rigid band model. Bonding in the partially negatively charged honeycomb Hg lattice may be approximately described by sp^2 hybridization and in the linear chains by sp hybridization. The breakup of $(Hg^{1/2+})_\infty$ chains into Hg_4^{2+} ions is derived from a Peierls distortion.

The electronic structures of several mercury compounds exhibit unusual properties, such as high electrical conductivity; some are even superconducting. Such is the case for the potassium graphite amalgams[1] $KHgC_4$ and $KHgC_8$. The former is a first-stage and the latter a second-stage Graphite Intercalation Compound, GIC.

The first-stage potassium amalgam GIC, $KHgC_4$, consists of alternating layers of carbon (A, B, ...), potassium (α, β, ...), and mercury (a, b, ...) whose layer stacking sequence is

$$A\alpha a\alpha A\beta b\beta A\gamma c\gamma A\delta d\delta A$$

Hg atoms occupy prismatic sites between potassium atoms as shown in Figure 1, which form a three-coordinated, almost planar, honeycomb network. The projected view of the crystal structure on the *a-b* plane is shown in Figure 1b.

The second-stage potassium amalgam GIC, $KHgC_8$, also has the same two-dimensional structure along the *a-b* plane but differs in the stacking sequence.

In this paper we discuss the electronic structure and bonding of these compounds together with the infinite-chain compounds $Hg_{3-\delta}MF_6$ (M = As, Sb, Nb, and Ta)[2,3] as well as the compounds Hg_3NbF_6 and Hg_3TaF_6.[2,4] The last two solids have close-packed Hg layers. What makes this structural diversity remarkable is that the formal electron count ranges from ~-0.5e in the graphite compounds to $\sim+^1/_3$e for the chain and layered compounds. The infinite-chain systems consist of incommensurate Hg chains in-

Table I. Summary of Calculations on $KHgC_{4n}$ (n = 1, 2)

syst	Fermi level, eV	ΔE,[a] eV	charge, e	
			Hg	C
$KHgC_4$ ("ideal")[b]	-9.77	0.213	-0.873	-0.020
$KHgC_4$ ("buckled")[b]	-9.76		-0.860	-0.020
$KHgC_8$ ("ideal")	-9.95	0.209	-0.824	-0.016
$KHgC_8$ ("buckled")	-9.87		-0.781	-0.020

[a] $\Delta E = E_{tot}/Hg$("ideal") - E_{tot}/Hg("buckled"). [b] "Buckled" refers to the actual buckled structure of the Hg network in the $KHgC_{4n}$ group (δ = 0.5 Å), whereas "ideal" refers to the planar, δ = 0 structure.

† Camille and Henry Dreyfus Teacher-Scholar (1984-1989).

(1) (a) Lagrange, P.; El Markini, M.; Guerard, D.; Herold, A. *Synth. Met.* **1980**, *2*, 191. (b) Herold, A.; Billaud, D.; Guerard, G.; Lagrange, P.; El Markini, M. *Physica B+C* **1981**, *105BB+C*, 253. (c) Alexander, M. G.; Goshorn, D. P.; Guerard, D.; Lagrange, P.; El Markini, M.; Ohn, D. G. *Synth. Met.* **1980**, *2*, 203. (d) Iye, Y. *Mater. Res. Soc. Symp. Proc.* **1983**, *20*, 185 and references therein. (e) Timp, G.; Elman, B. S.; Dresselhaus, M. S.; Tedrow, P. *Mater. Res. Soc. Symp. Proc.* **1983**, *20*, 201 and references therein. (f) Delong, L. E.; Yeh, V.; Eklund, P. C. *Solid State Commun.* **1982**, *44*, 1145.

(2) (a) Brown, I. D.; Cutforth, B. D.; Davies, C. G.; Gillespie, R. J.; Ireland, P. R.; Vekris, J. E. *Can. J. Chem.* **1974**, *791*, 51. (b) Schultz, A. J.; Williams, J. M.; Miro, N. D.; MacDiarmid, A. G.; Heeger, A. J. *Inorg. Chem.* **1974**, *17*, 646.

0020-1669/87/1326-2852$01.50/0

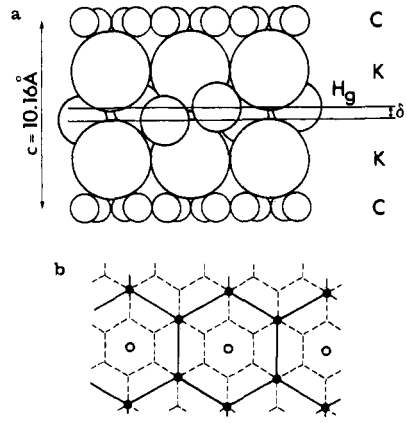

Figure 1. (a) Structure of the first-stage potassium amalgam graphite $KHgC_4$ (after Herold et al.[1b]). δ is the buckling parameter, found to be $\sim$0.5 Å. $\delta = 0$ corresponds to the model termed "ideal" in the text. (b) c-axis projection of the structure in (a): (O) K; (●) Hg; (---) graphite honeycomb.

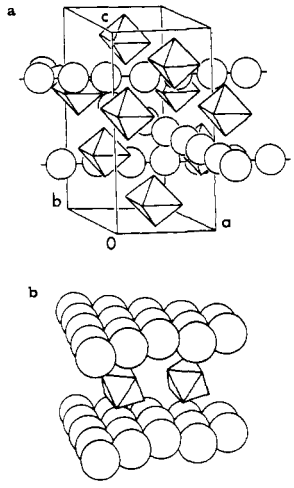

Figure 2. (a) Structure of the infinite-mercury-chain compound $Hg_{3-\delta}MF_6$ (after Brown et al.[3]). (b) Structure of the mercury layer compound Hg_3MF_6 (after Brown et al.[4]).

terpenetrating a lattice of MF_6^- anions (Figure 2a), while the Hg layers separate these anions in the layered compounds, as shown in Figure 2b. Zigzag chains with three shorter and one longer Hg–Hg bond occur in $Hg_4(AsF_6)_2$[5] and in $Hg_4(Ta_2F_{11})_2$.[3] We show in this paper that much of this variety in Hg–Hg bonding of these systems is due to their electronic structures.

1. Potassium Amalgam Graphite Intercalation Compounds

We have performed extended Hückel energy band calculations[6] on the actually observed structures of $KHgC_4$ and $KHgC_8$,[1] as well as on simplified models including only two layers of graphite and the amalgam sandwiched in between. The following issues were addressed: (a) the extent of validity of the rigid band model, advanced by Senbetu et al.,[7] for these GIC's; (b) the amount of charge transfer, q; (c) the energetics of the buckling of the Hg layer ($\delta = 0$ in Figure 1 corresponding to the model termed "ideal" and $\delta \approx 0.5$ Å to the experimental, "buckled", model); (d) the nature of the states (C, K, or Hg) at the Fermi level, E_F.

Before turning to the details of the electronic structure, we summarize the main results of the calculations on the $KHgC_{4n}$ ($n = 1, 2$) compounds in Table I. It is apparent that no electronic driving force to distort the "ideal" form has been identified. Furthermore, a remarkable similarity between the calculated results for the two compounds suggests that there may be very little interaction between the graphite layers and the amalgam layers. This was subsequently confirmed by two-dimensional (2D) layer calculations, which gave results very close to those of the full 3D ones. This justified the use of 2D models and provided numerical proof for the validity of the rigid band model. The main reason for the validity of the rigid band model is that the K(4s) orbitals are so extended that they provide very little overlap with the C(2p–π) states,[8] and the undulation of the states around the Fermi level is not in phase with any 4s-derived potassium states.[8b] The coefficients of the π orbitals at the Fermi level are illustrated in **1**. Their overlap with the potassium 4s orbital cancels due to the occurrence of pairs of opposite signs of these coefficients.

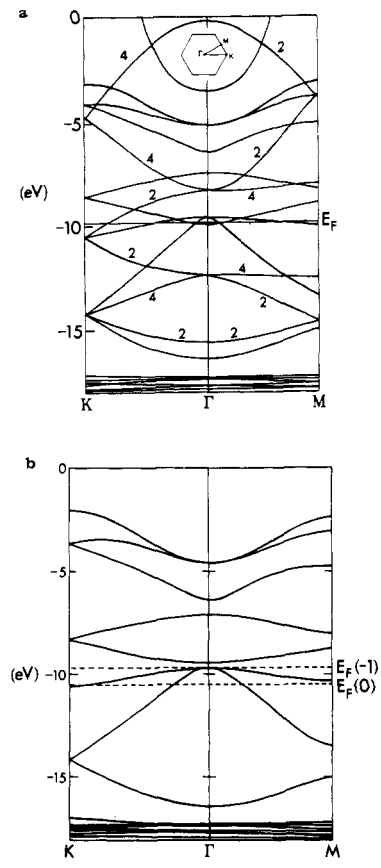

Figure 3. (a) Energy band structure of $KHgC_4$ from the experimental structure.[1b] The insert shows the notation of the Brillouin zone. E_F indicates the Fermi level. The numbers 2 and 4 indicate the degree of degeneracy of a band. (b) Energy band structure of a planar Hg honeycomb lattice. Numbers in parentheses are the charge per Hg.

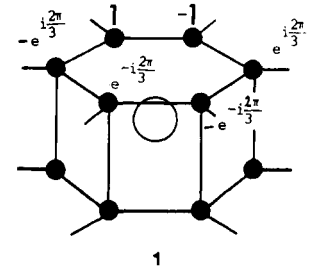

1

(3) Brown, I. D.; Datars, W.; Gillespie, R. J.; Morgan, K. R.; Tun, Z.; Ummat, P. K. *J. Solid State Chem.* **1985**, *57*, 34.
(4) Brown, I. D.; Gillespie, R. J.; Morgan, K. R.; Tun, Z.; Ummat, P. K. *Inorg. Chem.* **1984**, *23*, 4506.
(5) Cutforth, B. D.; Gillespie, R. J.; Ireland, P. R.; Sawyer, J. F.; Ummat, P. K. *Inorg. Chem.* **1973**, *22*, 1344.
(6) Whangbo, M. H.; Hoffmann, R.; Woodward, R. B. *Proc. R. Soc. London, A* **1979**, *366*, 23.
(7) Senbetu, L.; Ikezi, H.; Umrigar, C. *Phys. Rev. B: Condens. Matter* **1985**, *32*, 750.
(8) (a) Holzwarth, N. A. W. In *Graphite Intercalation Compounds*; Dresselhaus, M. S., Fisher, J. E., Moran, M. J., Eds.; North-Holland: Amsterdam, 1983. (b) Kertesz, M. *Int. J. Quantum Chem.* **1986**, *29*, 1165. (c) Inoshita, T.; Nakao, K.; Kamimura, H. *J. Phys. Soc. Jpn.* **1977**, *43*, 1237.
(9) Pitzer, K. S. *Acc. Chem. Res.* **1979**, *12*, 271. Pyykkö, P.; Desclaux, J. P. *Acc. Chem. Res.* **1979**, *12*, 276.

Good resonance of phases exists at $k = 0$ (this is the most bonding combination), but the energy separation between the K(4s) bonding and the C($2p\pi$) bonding states is too large ($\sim$10 eV) to permit appreciable mixing there either.

Let us now analyze the band structure of the compounds in some detail.

2. $KHgC_4$ Bands

The calculations show that the $KHgC_4$ bands below the Fermi level around −17 to −18 eV are mostly Hg(5d) with some K(4s) character. Figure 3a shows the calculated band structure of $KHgC_4$ along the K–Γ–M lines in the Brillouin Zone (BZ). There are 10 low-lying Hg 5d-like orbitals, and two bands have some 6s character at about −18.0 to −17.0 eV (note that the energy scale is shifted, as usual with EHT, to lower than the experimental values). The next band from below is mostly Hg(6s), and Hg(6p) with a small K(4s) character. There are three bands near the Fermi level (E_F) that are mainly of Hg(6p) character, in both the real ("buckled") and the "ideal" structures. At the Γ point the three bands are nearly degenerate, including a pair of $6p_x$ and $6p_y$ degenerate bands. In the "ideal" structure the third band ($6p_z$) lies above the degenerate pair while for the real structure the degenerate pair lies above the third band, because out-of-plane buckling destabilizes the mostly bonding $6p_z$ (π) orbital less than the σ-type $6p_x$ and $6p_y$. The two degenerate bands near the Fermi level split as we move away from the Γ point. On the other hand, the p_z band is pushed up in energy as we move away from the Γ point, similar to the case for the lower C($2p\pi$) band at Γ. Above the Hg(6p) bands are the antibonding bands of Hg(6s,6p). The potassium 4s bands are high up at around −2 eV.

In the real structure, at the Γ point, the energy difference between the p_z band and the degenerate pair is larger. In fact, the p_z band goes down in energy whereas the degenerate pair moves up slightly in energy. This stabilization of the p_z band is caused by the increased potassium–mercury interactions due to the decrease in the K to Hg distance. As a result there is greater K(4s) character in the real "buckled" structure than in the "ideal" structure. This can also be observed from the overlap populations between K and Hg (0.027 for the "ideal" and 0.047 for the real structures). The Hg–Hg bonding is not much affected by the buckling (0.494 for the "ideal" and 0.441 for the real structures). Although the overlap populations between K and Hg are small, the doubling of the value contributes to the said lowering of the $6p_z$ band.

The graphite bands remain largely unaffected by the K and Hg bands because of the absence of any significant mixing, as discussed above. The bands are similar to the graphite π bands from the calculations of previous workers zone-folded into the corresponding (one-fourth) Brillouin zone of $KHgC_4$.[7,8] The K(4s) bands are only slightly pushed up to higher energies by the graphite bands as was observed in comparing calculations for the bare KHg layer and $KHgC_4$, due to the large interplanar distance between the K layers and graphite as well as Hg layers and graphite. Thus, the band structure of $KHgC_4$ can be described as graphite bands superimposed on the Hg honeycomb band structure (Figure 3b) and a K(4s) band added on top. The calculations also show that there are no significant orbital mixings along the c axis. This means that there are no strong hybridization interactions between carbon layers, between carbon and KHg layers, and between intercalate layers.

3. $KHgC_8$ Bands—Two-Dimensional Model

Following the results of the $KHgC_4$ calculations, two-dimensional energy band calculations were done on $KHgC_8$. The bands are very similar to those of the $KHgC_4$ case and the Rigid Band Model (RBM) can be used to generate the band structure as well. There are three bands near the Fermi level. For the "ideal" structure, there are two degenerate bands at −9.69 eV (at Γ), one with Hg($6p_x$) and one with Hg($6p_y$). The other band at −9.61 eV has Hg($6p_z$) character. For the real or "distorted" structure, the same effect as in $KHgC_4$ was observed. That is, the band with mostly Hg($6p_z$) and a slight K(4s) character is shifted down in energy to −10.04 eV. The main difference is in the twice larger number of C layers for each analgam layer resulting in different degrees of charge transfer even within the RBM, because the graphite's and the analgam's Fermi levels are close.

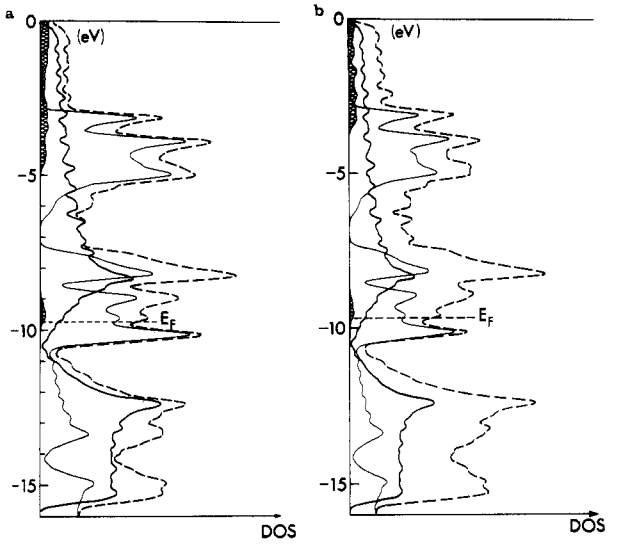

Figure 4. Density of states (DOS, total and projected) of (a) $KHgC_4$ and (b) $KHgC_8$: (broken line) total; (light solid line) Hg; (heavy solid line) C; (shaded region) K.

4. Density of States and Charge Transfer

Figure 4a shows the total density of states and projections to atomic states for $KHgC_4$. The Fermi level at −9.77 eV shows that $KHgC_4$ is metallic, with Hg states dominating at E_F. As to the DOS at the Fermi level, there are no significant differences between the "ideal" and the "buckled" structures. Most of the differences appear at energies above the Fermi level. Figure 4b shows the projected DOS of the three-dimensional calculation for $KHgC_8$. Comparing the DOS projections of the real buckled structure with the "ideal" one, we observed no significant differences and so we omitted the corresponding curves.

The charges on the atoms show that, for the ideal $KHgC_4$, 95.3% of the K charge goes to the Hg and graphite layers, with 93.0% going to the mercury layer. As for the real structure, 94.1% of the K charge goes to the Hg and graphite layers (86.3% to Hg). Most of the charge transferred to the mercury layers resides in the $6p_x$ and $6p_y$ orbitals. The charge on 6s is thus less than 2e; it is 1.57e, suggesting that the Hg honeycomb may be approximately described by sp^2 hybridization.

In $KHgC_8$, we observed that charge transfer from K to graphite is larger than in $KHgC_4$ (see Table I). This can be explained by the larger carbon to potassium ratio in $KHgC_8$ relative to that in $KHgC_4$. The nature of the states at E_F as well as the amount of charge transfer compare well with available experimental data.[1,10-14]

Optical reflectance showed[10] the presence of a strong absorption peak at 4.65 eV (our calculated value is 4.5 eV). The nature of these states is purely graphite π-like, strongly supporting the idea of survival of these states upon intercalation (rigid band model). Iye[1d] has concluded, on the basis of superconductivity data, that the majority of the charge carriers reside in the Hg bands rather than the graphite bands. This was further supported by the core level excitation spectra,[12] in agreement with our calculated DOS. The amount of CT was found to be slightly larger in the first-stage

(10) Heinz, R. E.; Eklund, P. *Mater. Res. Soc. Symp. Proc.* **1983**, *20*, 81.
(11) Fisher, J. E.; Fuerst, C. D.; Kim, H. J. *Mater. Res. Soc. Symp. Proc.* **1983**, *20*, 169.
(12) Preil, M. E.; Fischer, J. E.; Lagrange, P. *Solid State Commun.* **1982**, *44*, 357.
(13) Dicenzo, S. B. *Synth. Met.* **1985**, *12*, 25.
(14) Grunes, L. A.; Preil, M. E.; Ritsko, J. J.; Fischer, J. E. *Phys. Rev. B: Condens. Matter.* **1984**, *30*, 5852 and references therein.
(15) Albright, T. A.; Burdett, J. K.; Whangbo, M.-H. *Orbital Interactions in Chemistry*; Wiley-Interscience: New York, 1985.

compound than in the second-stage $KHgC_8$ by optical reflectance studies.[10] However, XPS results indicated[12,14] that there is more charge in the intercalate states in the second-stage than in the first-stage compound. Even though the calculated CT differs little in these two cases, our results indicate a somewhat larger amount of CT to the Hg states for $KHgC_4$ relative to that for $KHgC_8$.

The c-axis resistivity, ρ_c, is 7 times higher in $KHgC_4$ than in KC_8,[11] indicating an even smaller amount of s–π hybridization between the intercalate and carbon. Our calculations are not accurate enough to provide estimates for ρ_c.

Core level excitations indicated that the K(4s) states are unoccupied in both compounds.[12] Recent XPS studies of Di-Cenzo[13] on $KHgC_4$, $KHgC_8$, and KC_8 show an increasing occupancy of the K(4s) states in the sequence KC_8, $KHgC_8$, and $KHgC_4$. We find the following calculated charges on K by Mulliken population analysis (same sequence): 0.01e,[8] 0.02e, and 0.06e, respectively. Valence band spectra also suggest[13] a lower K(4s) occupation in $KHgC_8$ than in $KHgC_4$.

5. Bonding and Buckling in the Mercury Honeycomb

After surveying the evidence that the rigid band model, based on a negatively charged Hg honeycomb lattice, is approximately valid for the potassium amalgam GIC's, we now look at the mercury layer in some detail. The DOS curves of the $KHgC_{4n}$ compounds show that the DOS near the Fermi level is coming mostly from the mercury layer.

The interatomic distance between the Hg atoms in the honeycomb net in $KHgC_{4n}$ is 2.84 Å. This value is shorter than in elemental mercury and also shorter than the Hg–Hg distances (3.00–3.08 Å) in KHg_2,[16] the structure of which can be viewed as consisting of buckled honeycomb $Hg^{1/2-}$ layers connected by Hg–Hg bonds interspersed with K^+ ions in approximately hexagonal-prismatic holes.

The inter-mercury distance in the infinite-linear-chain $Hg_{3-\delta}AsF_6$ is shorter (2.67 Å) than the inter-mercury distance in the Hg hexagonal net. Similarly, the Hg–Hg distance in Hg_2^+ (2.54 Å) is shorter than that in the Hg honeycomb, as has been pointed out by Brown et al.[4]

The MO diagram of Hg_2^+ based on the extended Hückel scheme (see **2**) shows that the $2\sigma_g$ level of the valence molecular orbitals of Hg_2^+ is lower in energy than the $1\pi_g$ levels. This is

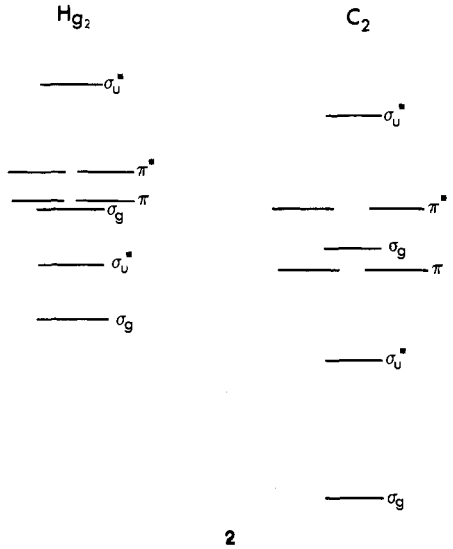

2

contrary to what is observed in B_2 and C_2. Also, s–p_x (σ) mixing is less pronounced in Hg_2 than in B_2 and C_2.[15] We would expect then that bonding in Hg_2^+ and in Hg_2^- would both be σ type but the bonding in the negative species would be less strong than that in the positive one, because the antibonding orbtial, $1\sigma_u$, is being filled before $2\sigma_g$. In the solid, however, these levels spread into bands, making an approximately sp^2 hybridization possible for a three-coordinated honeycomb lattice. (This structure can also be derived from that of $NaHg_2$, where no buckling of the honeycomb occurs[16] (AlB_2 type).[17])

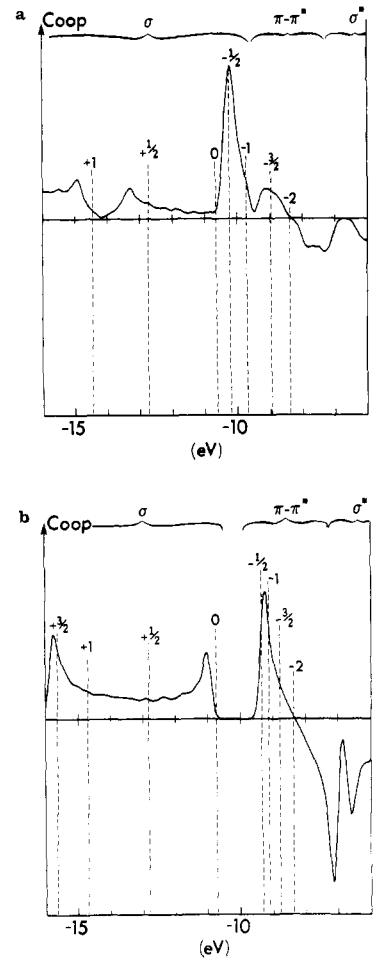

Figure 5. Crystal Orbital Overlap Population (COOP) curve for Hg systems: (a) Honeycomb structure; (b) equidistant linear chain. Indicated are the occupancies with different electron counts and the dominant symmetry of the corresponding orbitals.

The effects of relativity are important in the chemical properties of mercury.[9] These are indirectly refected in our parameters, but we believe that the 6s contraction would further weaken the s–p mixing and therefore lower $2\sigma_g$ in **2** even further. As is also expected, the 6p orbitals play a larger role in the bonding properties of mercury than the 5d orbitals.

One interesting question that could be asked is as follows: Why do negatively charged mercury atoms form honeycomb nets? Are reasons similar to the reasons carbon and boron form honeycomb nets? Analysis of the COOP (Crystal Orbital Overlap Population)[18a] curve of the Hg layer in Figure 5a reveals that there is more σ bonding between Hg atoms as they become successively more negatively charged. Bonding of negatively charged mercury atoms is somewhat similar to that of C^+ and B in honeycomb structures except that bonding in the mercury layer is due to a relatively larger contribution of the p orbitals. In a comparison of the COOP curves of the honeycomb layer with that of the equidistant linear chain (parts a and b, respectively, of Figure 5), the main difference is, of course, the presence of unfilled σ *and* π orbitals for the honeycomb, whereas for the chain only a pair of bands (e.g. π_x and π_y) is available. There is a gap of about

(16) Duwell, E. J.; Baenziger, N. C. *Acta Crystallogr.* **1955**, *8*, 705.

(17) (a) Buckling of AlB_2 type lattices have been recently analyzed in: Burdett, J. K.; Miller, G., submitted for publication. (b) The structure of Li_3In_2 (Stöhr, J.; Schäfer, H. *Z. Naturforsch., B: Anorg. Chem., Org. Chem.* **1979**, *34B*, 653) has buckled $In^{1.5-}$ honeycomb layers and can be related to the Hg^- honeycombs in $KHgC_{4n}$.

(18) (a) See e.g.; Hoffman, R. *Angew. Chem.*, in press. (b) See e.g.: Metzger, R. M. *J. Chem. Phys.* **1972**, *57*, 1870.

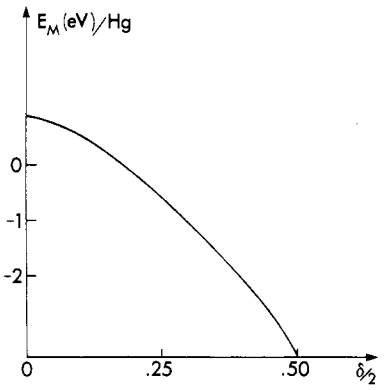

Figure 6. Madelung energy, E_M, of $KHgC_4$ as a function of the buckling parameter, $\delta/2$. δ is defined in Figure 1a; in $KHgC_4$ $\delta/2 \approx 0.25$.[16]

1 eV separating the unfilled bonding π states from the filled σ states in the neutral Hg chain, whereas no gap prohibits the acceptance of electrons in the honeycomb into σ-bonding states.

The buckling of the mercury layer in the potassium amalgam GIC's can be related to the electrostatic attraction between the positive potassium and negative mercury atoms. Figure 6 shows the electrostatic (Madelung) energy of $KHgC_4$, E_M, calculated by Ewald's method[18b] as a function of the buckling parameter, δ. This part of the energy is sharply decreasing as the structure is changed from the planar ($\delta = 0$) to the buckled form. Electrostatic considerations alone would favor a strongly buckled structure. However, buckling is limited by the presence of Hg–Hg bonds. Eventually, it is the interplay of electronic and electrostatic forces that on balance are responsible for the observed structure of the Hg layers in the potassium amalgam GIC's.

Since the structure of KHg_2, as well as $NaHg_2$, is related to the AlB_2 type, we may note that buckling is fairly common in this structure type. Burdett and Miller have recently discussed buckling of layers in a family of such systems, where they have correlated the buckling with metal–metal bonding between atoms around the honeycomb.[17] It seems that, in our case, classical electrostatic energy is driving the buckling, which is limited by the rigidity of the honeycomb sp^2 in-plane σ bonding.

6. Energetics of Different Hg Structures

It is tempting to consider the ranges of stability of the three competing structures (honeycomb, linear chain, and close-packed layer) as a function of the electron count. Assuming negligible interchain coupling in $Hg_{3-\delta}MF_6$, we have calculated the band structure of a Hg linear chain.[19] The calculated DOS is similar to that of more sophisticated calculations on $Hg_{3-\delta}AsF_6$ by de Groot et al.[20] The partially filled band of the linear mercury chain is consistent with the idea of partially positively charged mercury atoms and conduction due to the partially filled 6p (σ) band.

Figure 7 displays the pairwise energy differences, ΔE, as a function of formal charge on the mercury. The vertical lines indicate a given compound ($KHgC_4$ and $KHgC_8$ are indistinguishable on the given scale). The general trend seems to agree with experiment: the honeycomb structure is more stable for negatively charged Hg. KHg_2 and $NaHg_2$ fit into this picture, although in these systems the honeycombs are also connected to two neighboring ones by short Hg–Hg contacts. The energy difference of the close-packed vs. linear chains is very small for $\sim+^1/_3$-charged Hg. In this region the competition between metallic (close packed) and directed bonding using the remaining $\sim^5/_3$ valence electrons per Hg is apparently decided by factors too subtle to be caught by our simplified picture, which is usually not very good at discriminating among structures with a varying coordination number.

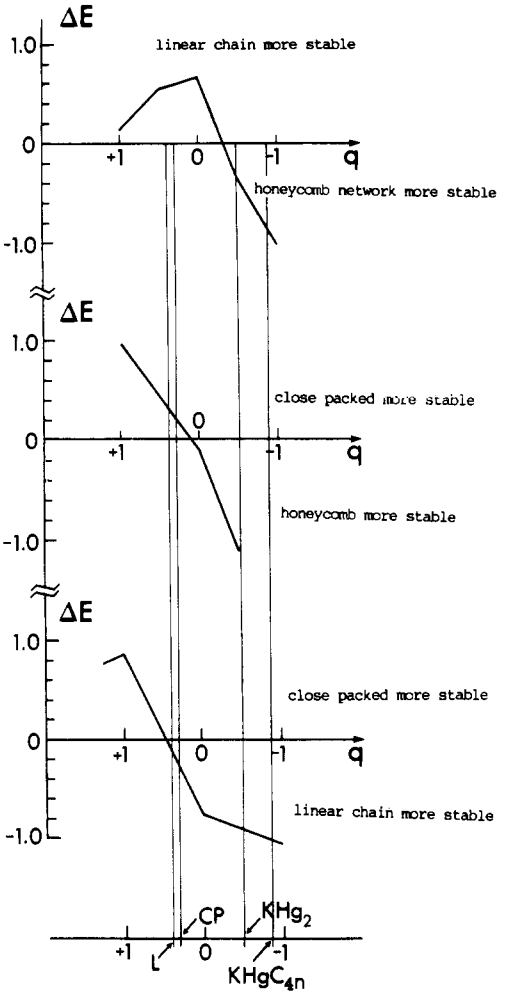

Figure 7. Energetics of Hg structures as a function of extra charge per Hg (q in eV/Hg): (L) Hg_3^+ linear chain; (CP) Hg_3^+ close-packed layer (lines provided to guide the eye).

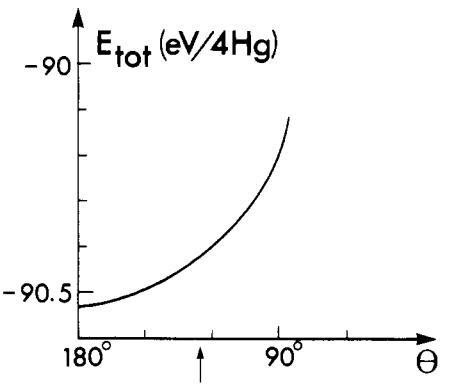

Figure 8. Total electronic energy per Hg in $(Hg_4^{2+})_\infty$ as a function of the zigzag angle, θ (defined in **3**). The arrow corresponds to the actual structure[5] in $Hg_4(AsF_6)_2$.

For a slightly more positively charged ($+^1/_2$) structure (Hg_4^{2+}), alternating zigzag chains are found experimentally. Let us derive this structure from an idealized equidistant Hg chain. The partial charge of +2 per four Hg atoms indicates a formal charge of $+^1/_2$ per Hg atom. Thus, to a good approximation, the 6σ band of the equidistant chain would be three-fourths filled. This immediately suggests a Peierls distortion, leading to quadrupling the unit cell.[21]

(19) Linear chains of main-group elements are rather rare. For the band structure of such systems, see e.g.: (a) Kertesz, M.; Koller, J.; Azman, A. *J. Chem. Phys.* **1978**, *68*, 2779. (b) Burdett, J. K. *Prog. Solid State Chem.* **1984**, *15*, 173. (c) Keszler, D. A.; Hoffmann, R. *J. Am. Chem. Soc.*

(20) (a) Buiting, J. J. M.; Weger, M.; Mueller, F. M. *Solid State Commun.* **1983**, *46*, 857. (b) De Groot, R. A.; Buiting, J. J. M.; Weger, M.; Mueller, F. M. *Phys. Rev. B: Condens. Matter* **1985**, *31*, 2881.

(21) Peierls, R. E. *Quantum Theory of Solids*; Oxford University Press: London, 1955; p 108.

Table II

atom	orbital	H_{ii}, eV	ξ_i	ref
C	2p	-11.4	1.625	6
K	4s	-4.34	0.87	8b,c
Hg	6s	-13.68	2.649	23
	6p	-8.47	2.631	
	5d[a]	-17.50	6.436 (3.032)	

[a] Exponents: $\xi_1 = 6.436$; $\xi_2 = 3.032$. Double-ζ expansion coefficients: $C_1 = 0.6438$; $C_2 = 0.5215$.

Analogously, polyiodides with a charge of $-^1/_3$ per iodine lead to the formation of I_3^- units as has been analyzed by Vondervisztand one of us[22] (unit cell trebling). The energy gain associated with this Peierls distortion is calculated by our EHT scheme to be 0.09 eV/Hg. This compares well[22] with the energy gain calculated for the trimerization of the $(I^{1/3-})_\infty$ chain (0.07 eV/iodine atom).

The angular deformation due to variations in θ (see **3**) costs some energy: according to band calculations we have performed for $(Hg_4^{2+})_\infty$ chains the most stable configuration occurs at $\theta = 180°$. However, the potential energy curve as a function of θ is soft (see Figure 8). The energy cost to deform the chain from

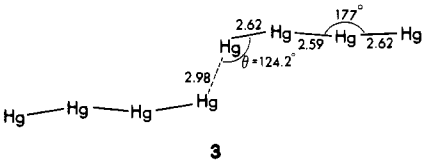

3

$\theta = 180°$ to the experimentally observed value[5] (124.2°) in $Hg_4(AsF_6)_2$, as indicated by an arrow in Figure 8, is only 0.03 eV/Hg. The potential energy curve in Figure 8 can be rationalized as follows. Due to $sp^{1-\delta}$ hybridization, a linear configuration is favored. Furthermore, if the p orbitals would not be involved at all, the electronic energy would depend on θ only very weakly. Due to the small s-p mixing, the calculated energy surface is still flat around $\theta = 180°$, as shown in Figure 8. Consequently, in further experimental studies of new Hg chains, a broad scatter of θ values is expected.

Acknowledgment. The financial support of the Camille and Henry Dreyfus Foundation is gratefully acknowledged. We are indebted to Ann Pope for the expert drawings and Kay Bayne for the typing.

Appendix

An extended Hückel crystal orbital method was used with the parameters given in Table II. The *k*-space integrations were performed with a 55-*k*-point set for the 2D calculations and a 165-*k*-point set for the 3D calculations.

(22) Kertesz, M.; Vondervisztt, F. *J. Am. Chem. Soc.* **1982**, *104*, 5889.
(23) Underwood, D. J.; Hoffmann, R.; Tatsumi, K.; Nakamura, A.; Yamamoto, Y. *J. Am. Chem. Soc.* **1985**, *107*, 5968.

Contribution from the Department of Chemistry, University of New Orleans, New Orleans, Louisiana 70148

^{13}C NMR Study of (*meso*-2,3-Butanediaminetetraacetato)nickelate(II)

Jan M. Robert and Ronald F. Evilia*

Received July 11, 1986

The temperature and pH dependences of the ^{13}C NMR spectrum of the paramagnetic nickel(II) complex with *meso*-2,3-butanediaminetetraacetic acid are reported and interpreted to indicate that the ligand acts as a hexadentate coordinator at all temperatures accessible in deuteriated water and over the pH range from 1 to 13. Less than 1% of the ligands act as pentadentate coordinators. The incomplete coalescence of acetate resonances coupled with concurrent complete coalescence of backbone resonances is interpreted to indicate that $\Delta \rightleftarrows \Lambda$ conversion proceeds rapidly at moderate (ca. 70 °C) temperatures through a symmetrical intermediate formed without bond breaking, while nitrogen inversion, which requires nickel-nitrogen bond rupture, is slow over the accessible temperature range (<109 °C). The previously proposed mechanism for the racemization of $Ni(EDTA)^{2-}$, which required the presence of an uncoordinated ligand arm, is probably incorrect. A mechanism is proposed that explains the previous and current data without invoking action by a free acetate arm. The *meso*-BDTA chelate ring is found to be more puckered than the chelate ring of EDTA. The pentadentate form of *meso*-BDTA is destabilized by at least 8 kJ mol^{-1} relative to the pentadentate form of EDTA because of steric interaction between a free carboxylate and the axial methyl substituent.

Introduction

Many workers have studied the coordination details of polydentate ligands. The amino carboxylate ligands have received considerable attention from many researchers using a variety of different techniques.[1-16] Although there has been some disagreement in the past, it appears that for ethylenediaminetetraacetic acid (H_4EDTA) coordinated to nickel(II) and other dipositive metal ions, the chelation involves hexadentate coordination by approximately two-thirds of the EDTA molecules and pentadentate coordination by the remaining one-third of the EDTA molecules.[11,16] The thermodynamic values ΔH and ΔS for the pentadentate $\rightleftarrows$ hexadentate equilibrium have been measured for the complexes $Ni(EDTA)^{2-}$ and $Ni(1,2\text{-}PDTA)^{2-}$.[16]

A recent report has confirmed an earlier study which concluded that when a methyl group is substituted onto the EDTA backbone to produce the ligand 1,2-propylenediaminetetraacetic acid (H_4-1,2-PDTA), the percentage of pentadentate coordination is reduced to half that of the EDTA complex. When a cyclohexane ring composes the backbone as in the ligand 1,2-cyclohexanedi-

(1) Jørgensen, C. K. *Acta Chem. Scand.* **1955**, *9*, 1362-1377.
(2) Higginson, W. C. E. *J. Chem. Soc.* **1962**, 2761-2763.
(3) Bhat, T. R.; Krishnamurthy, M. *J. Inorg. Nucl. Chem.* **1963**, *25*, 1147-1154.
(4) Margerum, D. W.; Rosen, H. M. *J. Am. Chem. Soc.* **1967**, *89*, 1088-1092.
(5) Krishman, K.; Plane, R. A. *J. Am. Chem. Soc.* **1968**, *90*, 3195-3200.
(6) Brunetii, A. P.; Nancollas, G. H.; Smith, P. N. *J. Am. Chem. Soc.* **1969**, *91*, 4680-4683.
(7) Wilkins, R. G.; Yelin, R. E. *J. Am. Chem. Soc.* **1970**, *92*, 1191-1194.
(8) Matwiyoff, N. A.; Strouse, N. A.; Morgan, L. O. *J. Am. Chem. Soc.* **1970**, *92*, 5222-5224.
(9) Erickson, L. E.; Young, D. C.; Ho, F. F.-L.; Watkins, S. R.; Terrill, J. B.; Reilley, C. N. *Inorg. Chem.* **1971**, *10*, 441-453.
(10) Young, D. C.; Reilley, C. N. *Coord. Chem.* **1971**, *1*, 95-105.
(11) Grant, M. W.; Dodgen, H. W.; Hunt, S. P. *J. Am. Chem. Soc.* **1971**, *93*, 6828-6831.
(12) Everhart, D. S.; Evilia, R. F. *Inorg. Chem.* **1975**, *14*, 2755-2759.
(13) Howarth, O. W.; Moore, P.,; Winterton, N. *J. Chem. Soc., Dalton Trans.* **1975**, 360-368.
(14) Everhart, D. S.; Evilia, R. F. *Inorg. Chem.* **1977**, *16*, 120-125.
(15) Harda, S.; Funaki, Y.; Yasunaga, T. *J. Am. Chem. Soc.* **1980**, *102*, 136-139.
(16) Evilia, R. F. *Inorg. Chem.* **1985**, *24*, 2076-2080.
(17) Sudmeier, J. L.; Reilley, C. N. *Anal. Chem.* **1964**, *36*, 1707-1712.

0020-1669/87/1326-2857$01.50/0